CHAPTER - IV

STRUCTURAL, OPTICAL AND ELECTRICAL PROPERTIES OF SPRAYED MOLYBDENUM OXIDE THIN FILMS

CHAPTER-IV

STRUCTURAL, OPTICAL AND ELECTRICAL PROPERTIES OF SPRAYED MOLYBDENUM OXIDE THIN FILMS

4.1 INTRODUCTION

The transition metal oxides form a group of predominantly ionic solids which exhibit a wide range of optical and electrical properties. Many of these oxides have considerable use in electronic and magnetic devices, in heterogeneous catalysis [1] and number of other applications.

Molybdenum trioxide is a transparent partially ionic 4d transition metal oxide, which can be prepared in thin film form by using broad variety of techniques (given in section 1) with a view to use them in photochromic cell, electrochromic cell, image recording and holography. However preparation of MoO_3 films by using spray pyrolysis techniques and their structural, electrical and optical properties are studied for the first time.

This chapter presents, structural, optical and electrical properties of MoO_3 films. The effect of substrate temperature on these properties are studied. The substrate temperature was varied from 250° to 450°C. The films deposited on to amorphous glass substrate.

4.2 EXPERIMENTAL

4.2.1 THICKNESS MEASUREMENT

Film thickness is an important parameter in the study of the film properties. Amongst different methods for measuring the film thickness, the weight difference method is simple and convenient. The thickness 't' is measured using the relation.

$$t = m/A \varrho_b \qquad .....(4.1)$$

where 'm' is the mass of the film deposited on area 'A' of the substrate and 'ϱ_b' is the density of bulk material.

4.2.2 X-RAY DIFFRACTION

X-ray diffraction technique is useful tool for structural investigations [2]. This technique, based on monochromatic radiation is important becaus the 'd' spacings can be calculated from the observed diffraction angles. In diffractometer, the diffracted radiation is detected by a counter tube which moves through an angular range of reflections. The intensities are recorded on synchronously advancing strip-charts.Philips PW-1710 X-ray diffractometer, using CuK_α radiation with wavelengths ($\alpha_1\alpha_2$): 1.54060 A^o, 1.54438 A^o was used. The X-ray tube was operated on 25 KV, 20 mA. The XRD patterns for the films were recorded within the span of angles 20 to 80^o.

4.2.3 SURFACE MORPHOLOGY

Surface morphology of the MoO_3 thin films has been examined using scanning electron microscopy. Surface morphology of the films has been observed from scanning electron micrographs taken with the help of scanning electron microscope, Cambridge stereoscan 250 ,MK-3 unit. This helps to study the microstructure of the surface of the thin films.

4.2.4 OPTICAL ABSORPTION SPECTROSCOPY

The films prepared were analysed by the optical absorption studies. The variation of optical absorption density ' αt' with wavelength 'λ' for the films were carried out, in the wavelength range 350 to 850 nm with Hitachi 330 spectrophotometer. This data were further analysed for the estimation of the band gap energy.

4.2.5 ELECTRICAL RESISTIVITY

Resistivity measurement methods cover the entire range of contact and non-contact approaches and studied by various authors [3-8]. In this study, the two probe method was used for d.c. electrical resistivity measurement in the temperature range 400 to 600 K. The area of the films was defiend and silver paste was applied to ensure good ohmic [9] contacts to the film. A battery charger (30 V,6A) was used to pass current through the fim and high impedance voltmeter was used for the voltage measurement across the film sample. The size of the film was

1 X 1 cm^2. To study temperature dependent resistivity measurement, strip type heaters (65 W) were used to heat the samples and chromel-Alumel thermocouple was used to measure the temperature. Temperature was controlled with ± 2 ^oC accuracy usign APLAB temperature controller.

4.3 RESULTS AND DISCUSSION

Ammonium molybdate solution was sprayed on to preheated glass substrates. It undergoes pyrolytic decomposition and results in to the formation of thin solid MoO_3 films. The chemical reaction for the MoO_3 film formation is given in section (3.3.2). The films prepared at different substrate temperatures are denoted by S_{250}, S_{300},S_{350},S_{400} and S_{450}, where subscripts dentoes the substrate temperatures in degree centigrades.

4.3.1 THICKNESS MEASUREMENTS

Thickness of the films prepared at different substrate temperatures were measured and the variation is shown in figure 4.1. The film thickness decreases continuously with increasing substrate temperature. Similar types of results have been obtained for sprayed oxide and chalcogenide films. This behaviour is attributed to the increase in evaporation rate of initial product before reaching to the substrates, with increasing substrate temperature [10,11,12].

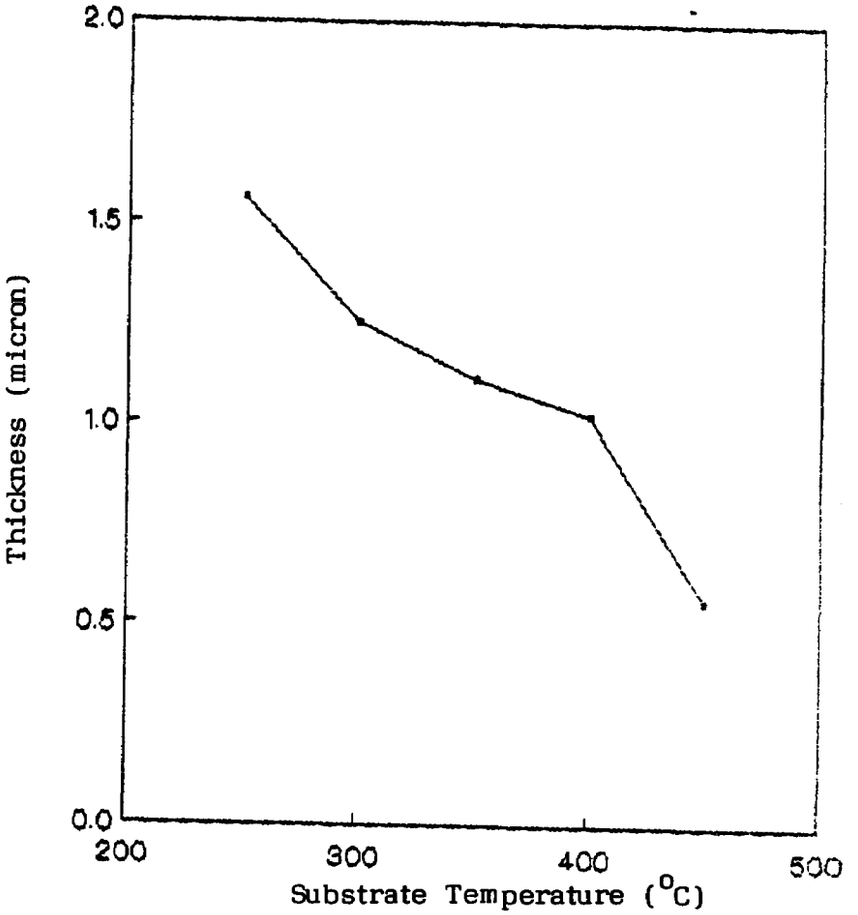

Fig. 4.1 : Variation of Film Thickness with Substrate Temperature

4.3.2 X-RAY DIFFRACTION

The film crystallography was determiend from XRD patterns. Fig.4.2 (a,b,c,d and e) shows XRD patterns of MoO_3 films prepared at different substrate temperatures. It is observed that the films deposited at temperatures 250°C and 300°C are amorphous (Fig.4.2 a and b), while the crystallization of the films was found to begin above 300°C. The films deposited at substrate temperatures between 350°C to 450°C were polycrystalline with preferred orientation in (210) plane, Fig.4.2 (c,d and e). Similar results have been reported for WO_3 films prepared by spray pyrolysis and d.c. magnetron sputtering methods [13,14].

The 'd' values of planes were calculated and compared with standard 'd' values taken from ASTM data files (Table 21.569) and are listed in Table 4.1. For amorphous films the 'd' values were calculated for the peaks having more dominant counts than the background counts and the observed 'd' values were compared with standard 'd' values and the composition of these films was found to be mainly of MoO_3.

The films deposited at substrate temperatures 250°C and 300°C were subjected to annealing at 500°C for 6 hours in air and analysed by XRD. Both the films became polycrystalline as shown in Fig.4.3(a and b) respectively, for S_{250} and S_{300} with preferred orientation in (100) and (210) planes respectively.

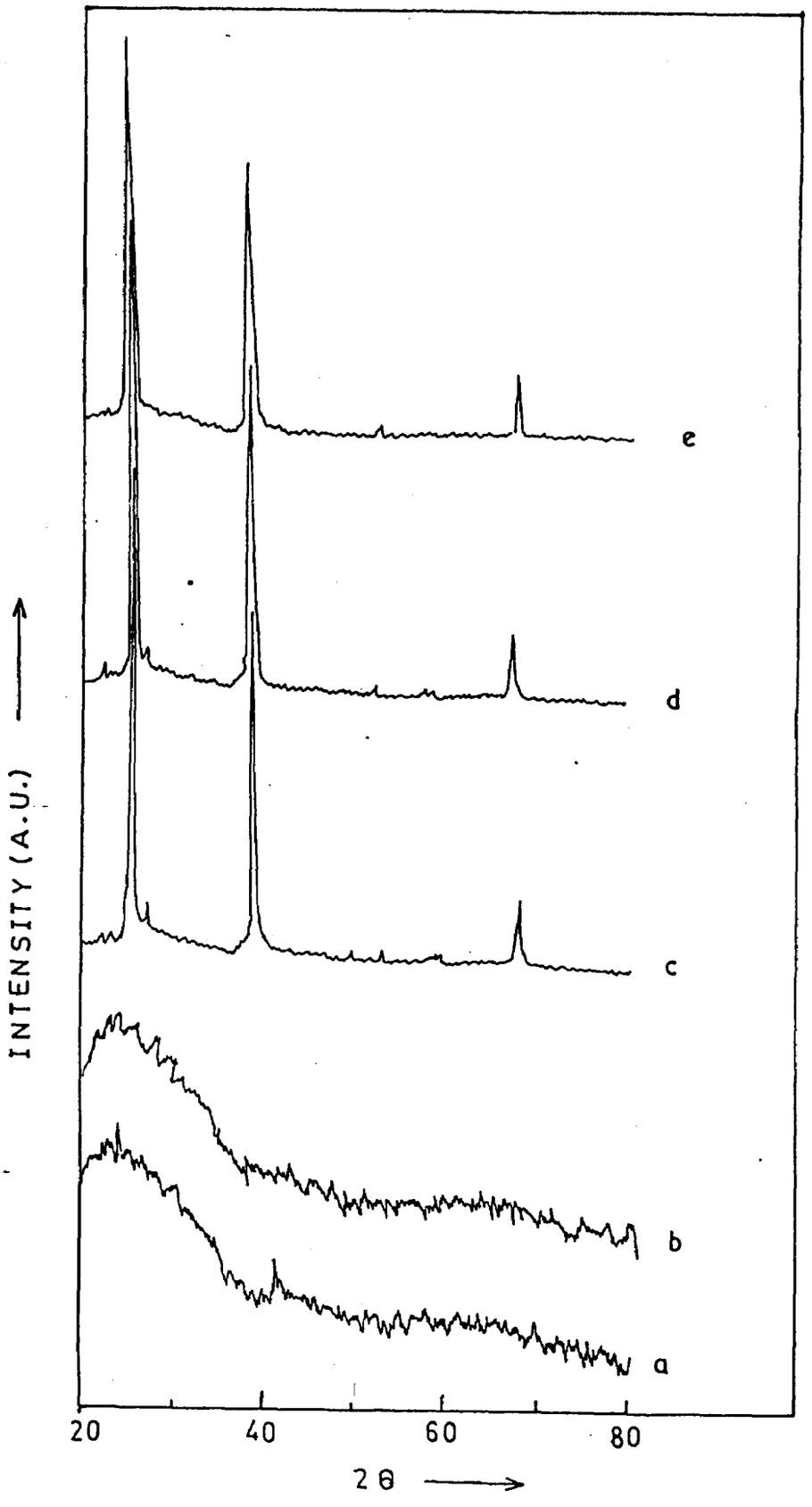

Fig.Fig.4.2 (a,b,c,d and E) : XRD Patterns of MoO_3 Films Prepared at Different Substrate Temperatures.

Table 4.1 Comparison between standard and observed "d" values

Sr. No.	Standard "d" values in A^{o}	Observed "d" values in A^{o}	I/I_{max} %	Plane (hkl)
S_{250}				
1	3.58	3.5766	44.92	---
2	2.147	2.147	77.1	224
S_{300}				
1	3.26	3.2659	54.96	---
2	3.16	3.1874	103.48	---
3	2.10	2.10	65.67	---
S_{350}				
1	3.80	3.84	0.33	---
2	3.45	3.4729	100.00	210
3	3.26	3.2641	2.06	---
4	2.34	2.3159	58.12	---
5	2.298	2.3096	42.63	---
6	1.86	1.8474	0.43	008
7	1.75	1.7361	0.64	330
8	1.63	1.65	0.36	218
9	1.56	1.5688	0.60	424
10	1.44	1.4438	0.40	---
11	1.39	1.3888	5.59	610
12	1.23	1.23	0.48	(3011)
S_{400}				
1	3.45	3.4702	99.76	210
2	3.26	3.2606	1.69	---
3	3.02	3.025	0.38	---
4	2.34	2.3139	59.16	---
5.	1.86	1.848	0.38	(008)
6	1.724	1.7324	0.59	(420)
7	1.584	1.5830	0.50	---
8	1.392	1.3891	5.27	(610)
9	1.207	1.2187	0.50	(1112)
S_{450}				
1	3.45	3.4696	100	210
2	2.348	2.3122	60.91	---
3	1.739	1.7324	0.93	---
4	1.392	1.3866	7.59	610

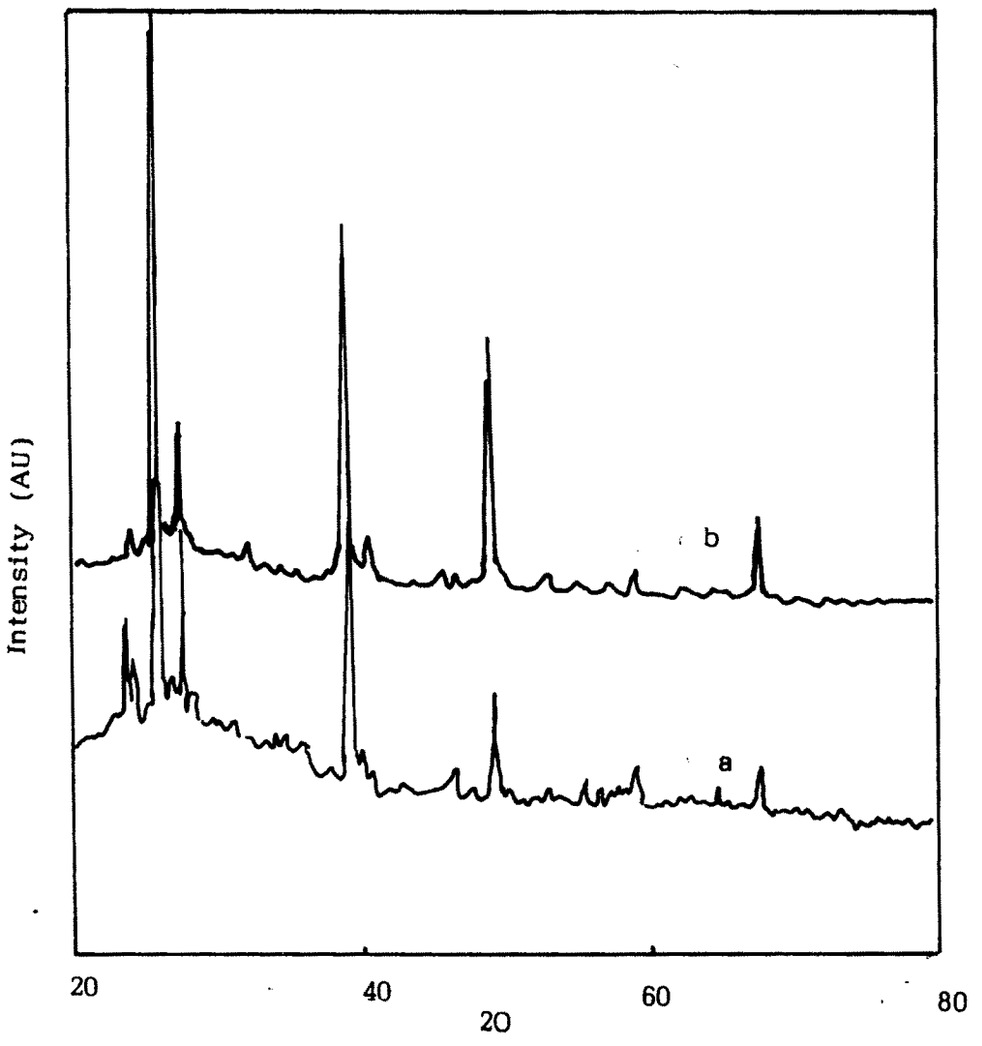

Fig.4.3 : XRD Pattern After Anealing of Films
a) S_{250} (b) S_{300}

4.3.3 SURFACE MORPHOLOGY

The scanning electron micrographs of the films prepared at substrate temperatures 350 and 400°C with (5000×) and (7000×) magnifications are shown in Fig.4.4 (a and b) respectively. Fig.(4.4a) reveals that, film surface is smooth and continuous while Fig.(4.4b) shows that the film surface is rough, full with flake like structure and the film is continuous. Such type of surface structure is an artifact of spray pyrolysis method.

4.3.4 OPTICAL ABSORPTION MEASUREMENT

The optical density (αt) of the film was recorded in the wavelength range of 350 to 650 nm at 300 K. The values of α were not corrected for the transmittance and reflectance of the film surface. The optical data were analysed from the following classical relation for near edge optical absorption in a semiconductor

$$\alpha = K(h\nu - Eg)^{n/2}/h\nu \qquad \ldots\ldots (4.2)$$

where 'K' is constant, 'Eg' is a semiconductor band gap and 'n' is constant equal to 1 for direct gap and 4 for indirect gap compound [15].

In order to confirm the nature of optical transition in MoO_3 film the plots of $(\alpha h\nu)^2$ versus $(h\nu)$ and $(\alpha h\nu)^{1/2}$ versus $(h\nu)$ were studied and shown in Fig.4.5 for a typical film. Linear portion of the curve was observed for

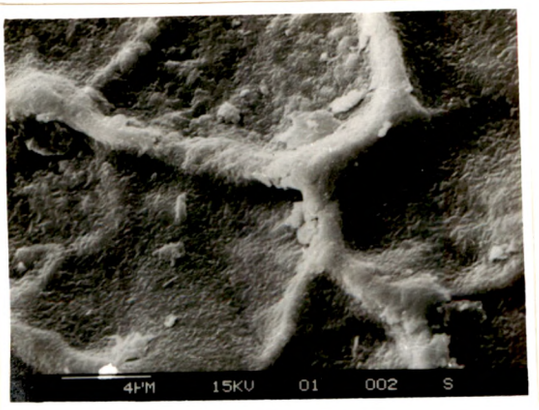

(5000 x)

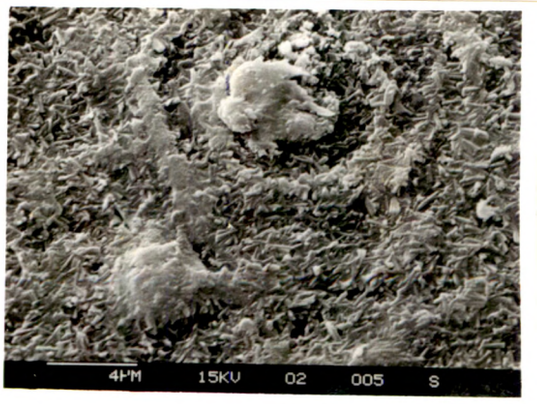

(5000 x)

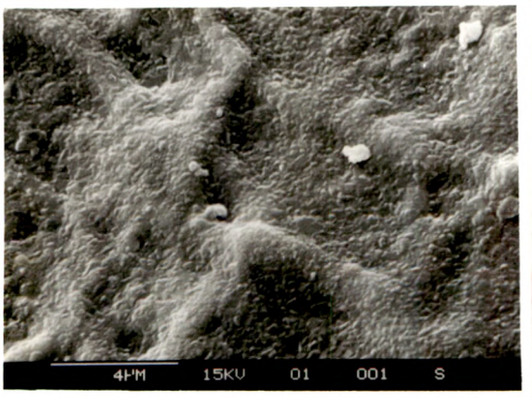

(7000 x)

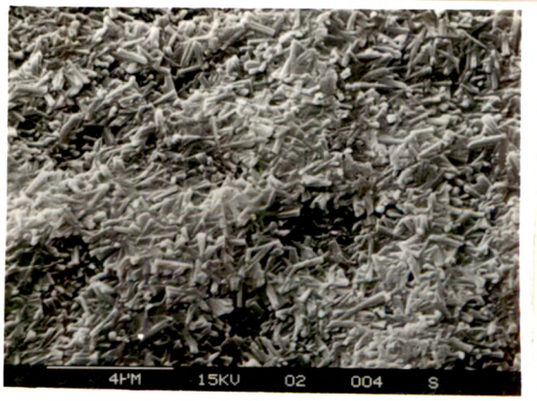

(7000 x)

a) SEM of the film S_{350}

b) SEM of the film S_{400}

Fig.4.4

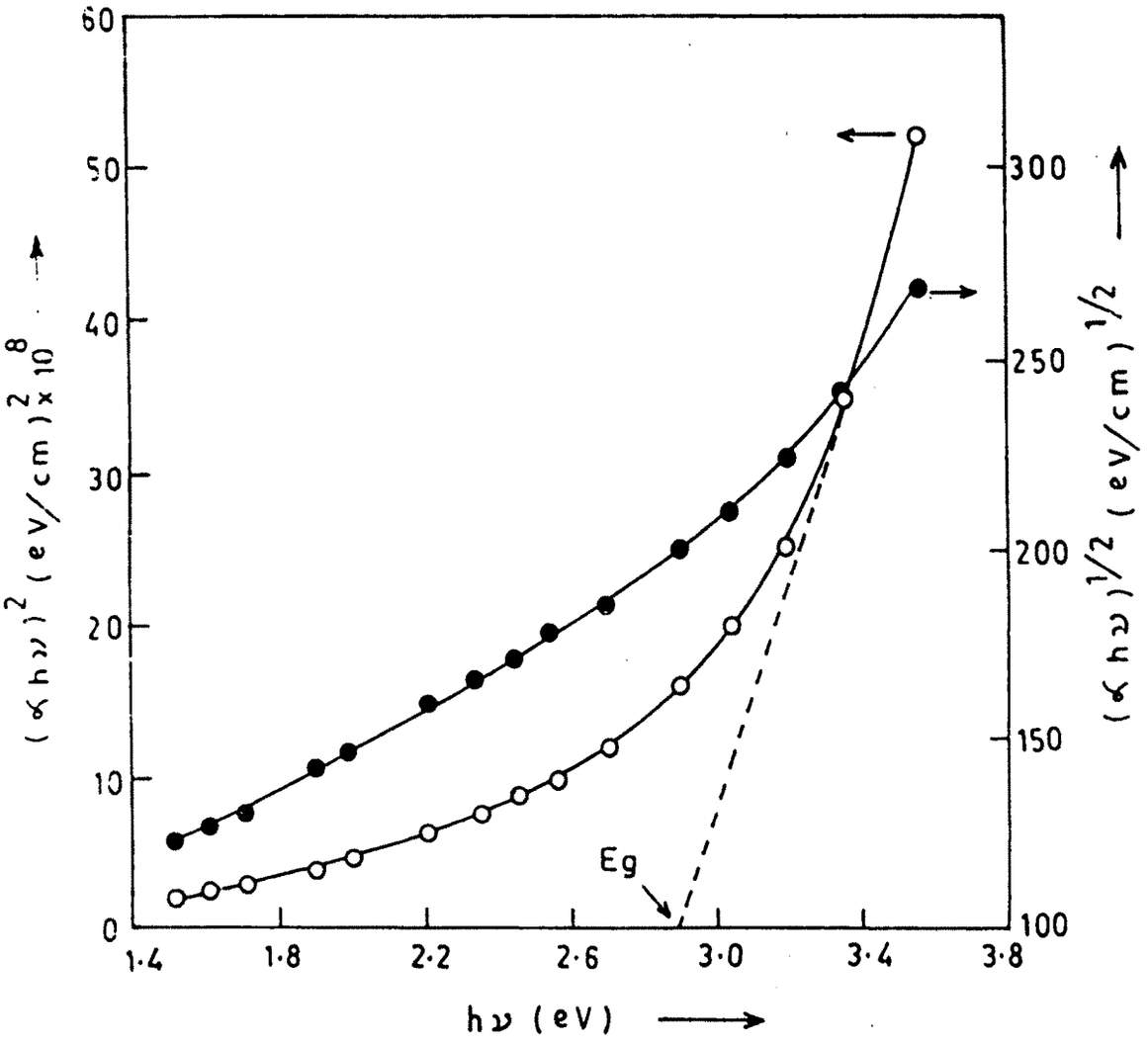

FIG·4.5 – PLOTS OF $(\alpha h\nu)^2$ Vs $h\nu$ AND $(\alpha h\nu)^{1/2}$ Vs $h\nu$ FOR MoO_3 THIN FILMS.

the plot of $(\alpha h\nu)^2$ versus $(h\nu)$ and extrapolation of this portion to zero absorption coefficient gives optical band gap energy equal to 2.97 eV. However, estimation of band gap energy from the plot of $(\alpha h\nu)^{1/2}$ versus $(h\nu)$ was outrageous. This observation therefore leads to the conclusion that the optical absorption in MoO_3 film takes place through direct interband transition. In a discrete MoO_6 ; it is apparent that the 5p,5s and 4d (e_g) orbitals of the central atom can combine with the six SP hybrid orbitals of the oxygen atoms, (one per atom) to give a set of six bonding σ and six anti-bonding σ^* molecular orbitals. In an extended lattice the discrete energy levels arising from this structure unit will broaden into bands. In addition, the molyubdenum 4d (t_{2g}) orbitals can combine with three of the surrounding oxygen $p\pi$ orbitals per octahedron to form bonding π and anti-bonding π^* bands. This leaves three oxygen $p\pi$ orbitals per octahedron which are of the wrong symmetry to combine with any of the molybdenum orbitals and which therefore remain as non-bonding levels ($p\pi^+$). The band structure arising from this qualitative discussion is shown in Fig.4.6. There are 24N valance electrons per mole of MoO_3 (where N is Avogadro's number) and if these are allocated to the successive bands shown in Fig.4.6, they will occupy 12N levels of lowest energy; i.e. the σ and π bands and the oxygen $P\pi^+$ levels will be completely full. This combination constitutes the valance band. The π^* and σ^* bands are empty and former becomes the conduction band in MoO_3.

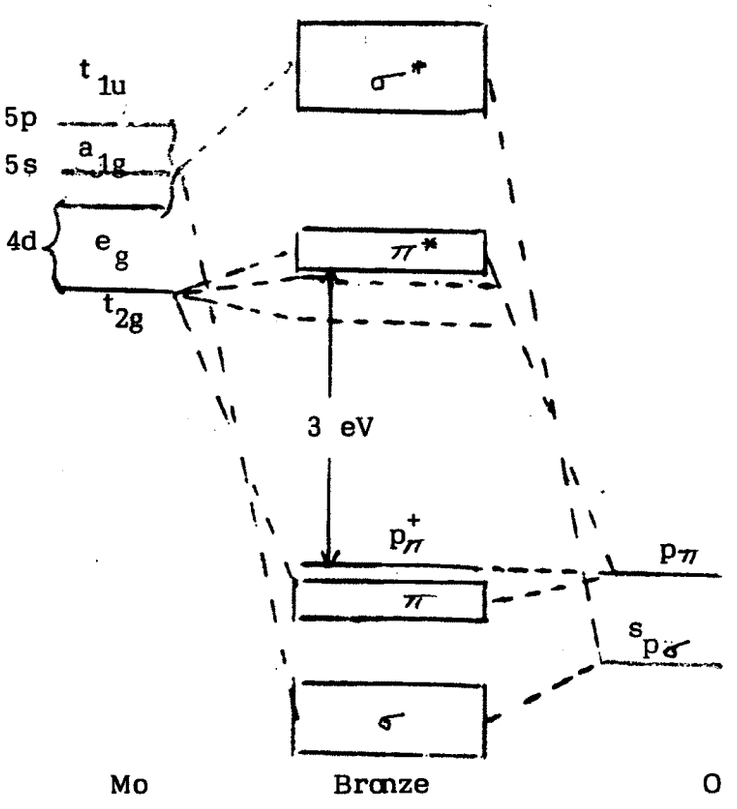

Fig.4.6 : Electronic Energy Level diagram for the Molybdeum Bronzes --.--.-- Donor Levels in Metallic Conductors ; ---- Donar Levels in Semiconductors.

The absorption edge in the spectrum of MoO_3 is thus associated with the onset of promotion of electrons from the $p\pi^+$ into the π^* band and the energy gap between the valence and condution bands is assigned a value of 2.96 eV as shown in Fig.4.6. This value decreases slightly (0.2 eV), when MoO_3 is oxygen deficient and similar effect is also observed for the bronzes [16,17].The value of band gap energy in the present study is in good agreement with the above value.

The variation of optical density (αt) with wavelength 'λ' for all the films is shown in Fig.4.7. The absorption coefficient is of the order of 10^4 cm^{-1} and a steep absorption rise was observed on the shorter wavelength side. Similar behaviour was observed for all the films. The recorded optical data were analysed for both possible direct allowed and direct forbidden optical transitions.

The quantitative optical band gap energy (Eg) can be derived by applying following relation

$$(\alpha h\nu) = (h\nu - Eg)^n \qquad \ldots\ldots\ldots (4.3)$$

where 'n' in the above equation depends on the kind of optical transitions that prevail. Specifically, n is 1/2, 3/2, 2 and 3 for transitions being direct allowed, direct forbidden, indirect allowed and indirect forbidden respectively [14].

Above results corroborated direct inter-band

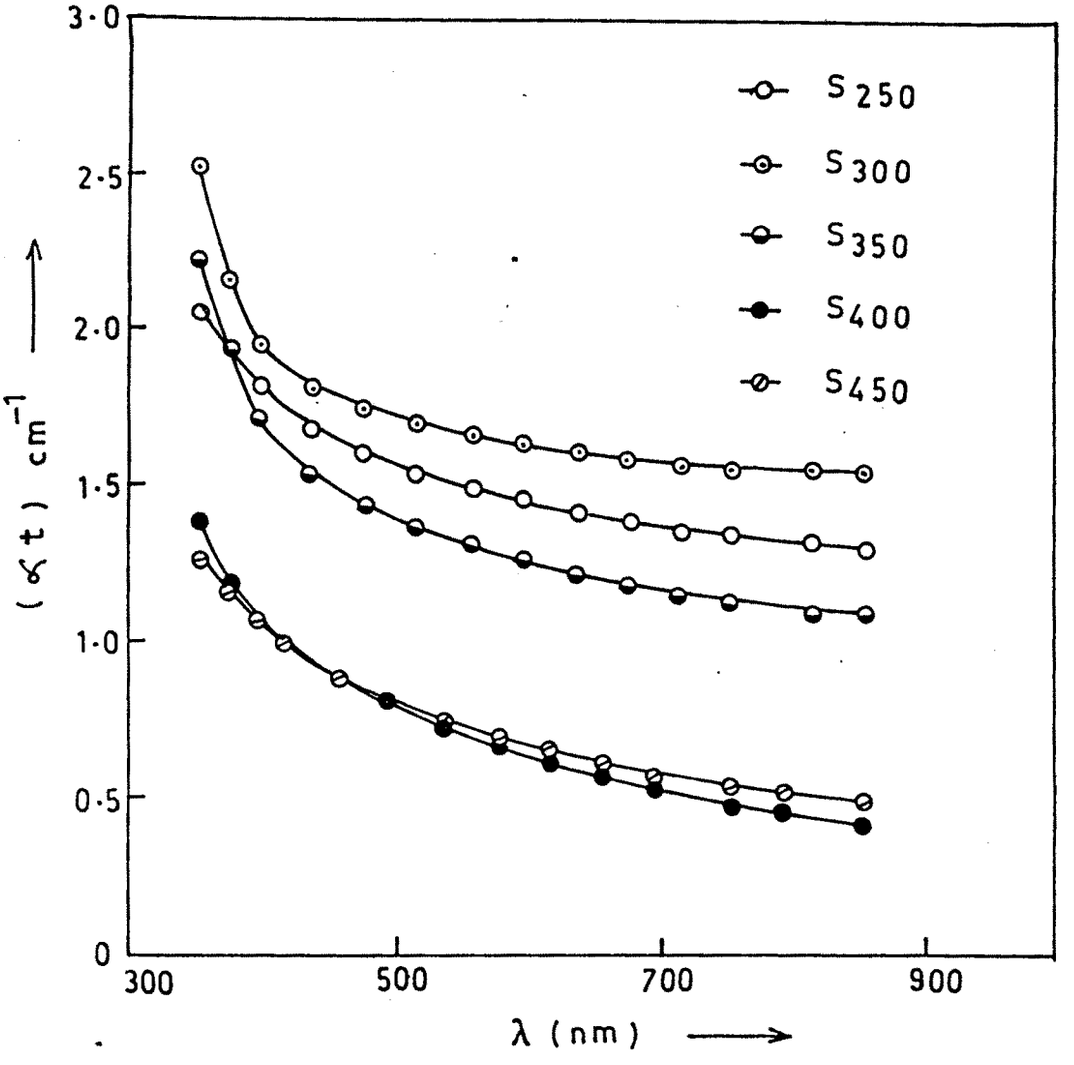

FIG.4.7– PLOT OF (αt) VERSUS (hν).

optical transitions in spray pyrolysed MoO_3 films; suggesting the absence of indirect transitions. Therefore, the optical data were further investigated for evidence of direct forbidden transitions.

Fig.4.8 shows variation of $(\alpha h\nu)^2$ versus $(h\nu)$ for all the films. Extrapolation of these curves to zero absorption coefficient gives the optical band gap energy (Eg), equal to 2.60 eV, 2.97 eV, 2.97 eV, 2.97 eV, and 2.82 eV for the film samples S_{250}, S_{300}, S_{350}, S_{400} and S_{450} respectively.

The data were also checked for the possibility of forbidden direct transitions in which $(\alpha h\nu)^{2/3}$ versus $(h\nu)$ is plotted for all films and shown in Fig.4.9. Extrapolation of these curves to zero absorption coefficient leads to band gap energies of 1.05 eV, 2.05 eV, 2.05 eV, 2.05 eV and 1.58 eV for S_{250}, S_{300}, S_{350}, S_{400}, S_{450} respectively suggesting direct forbidden transitions at these energies in MoO_3 thin films.

4.3.5 ELECTRICAL RESISTIVITY

The dark resistivity (ρ) is measured at room temperature (27°C) for all the films and listed in Table 4.1. It is observed that (ρ) was of the order of 10^6 to 10^7 ohm-cm for S_{250} and S_{300}, while it is of the order of 10^3 ohm-cm for S_{350} and S_{400} films. This may be due to the improved crystallinity of the films at higher substrate temperatures.

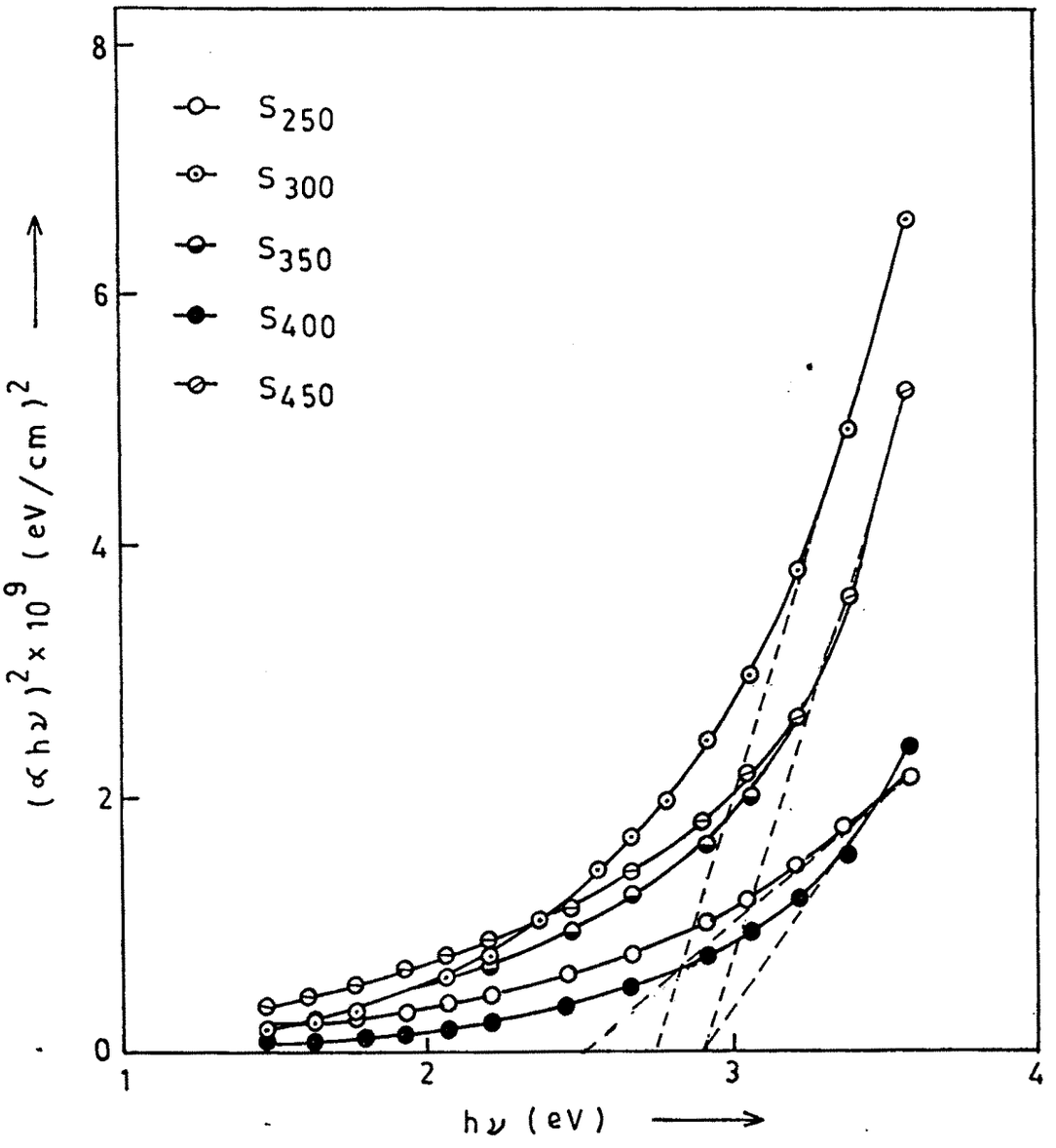

FIG.4.8— PLOT OF $(\alpha h\nu)^2$ VERSUS $(h\nu)$.

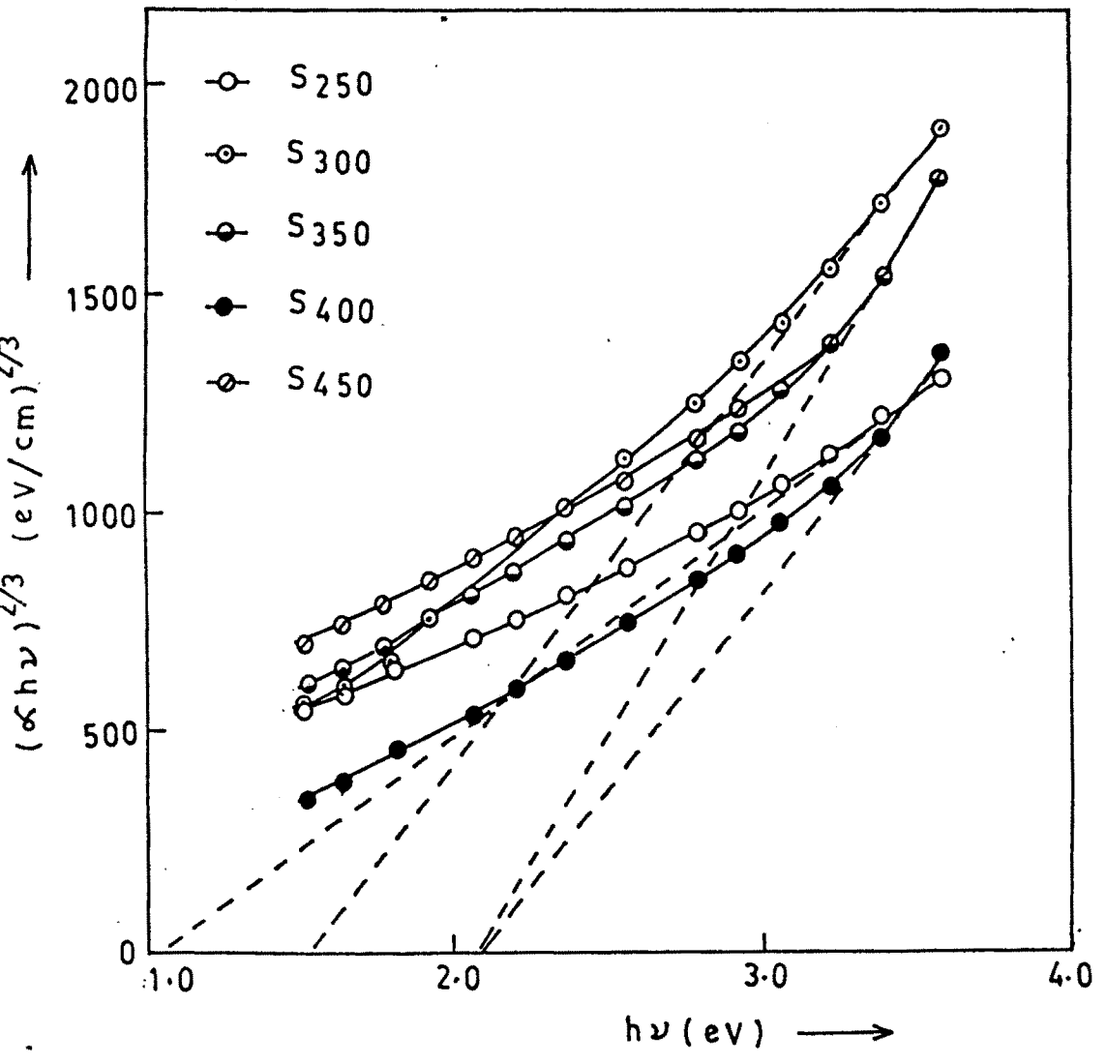

FIG.4.9— PLOT OF $(\alpha h\nu)^{2/3}$ VERSUS $(h\nu)$

Table 4.2 Variation of film thickness resistivity and activation energy with substrate temperature

Substrate temperature °C	Film Thickness μ	Room temperature resistivity ohm-cm	Activation Energy in eV	
			Low temp.	High temp.
250	1.56	6.6×10^7	0.32	0.25
300	1.25	9.12×10^6	0.31	0.19
350	1.11	8.31×10^3	0.18	0.06
400	1.02	2.88×10^3	0.09	0.05
450	0.56	-	-	-

Fig.4.10 shows the plot of log ρ versus reciprocal of the absolute temperature for all the films. The plot consists of two regions, giving two activation energies corresponding to low and high temperature regions. From both regions, thermal activation energies (E_a) are determined using the resistivity relation,

$$\rho = \rho_o \exp(-E_a/kT) \quad - - - - - (4.4)$$

where, ρ_o is a constant, 'k' is Boltzman's constant and T is absolute temperature. Activation energy represents the average energy of the carriers with respect to the Fermi energy, if the carriers can only move at the bottom or top of the well defined band. Presence of such two activation energies have been also shown by others for MoO_3 films prepared by physical vapour deposition [18].

The values of activation energies in the low and high temperature regions increases with increase in the film thickness and hence with decrease in substrate temperature as given in Table 4.2. This may be due to the combined effects of variations in crystallinity and dislocation density, [18, 19].

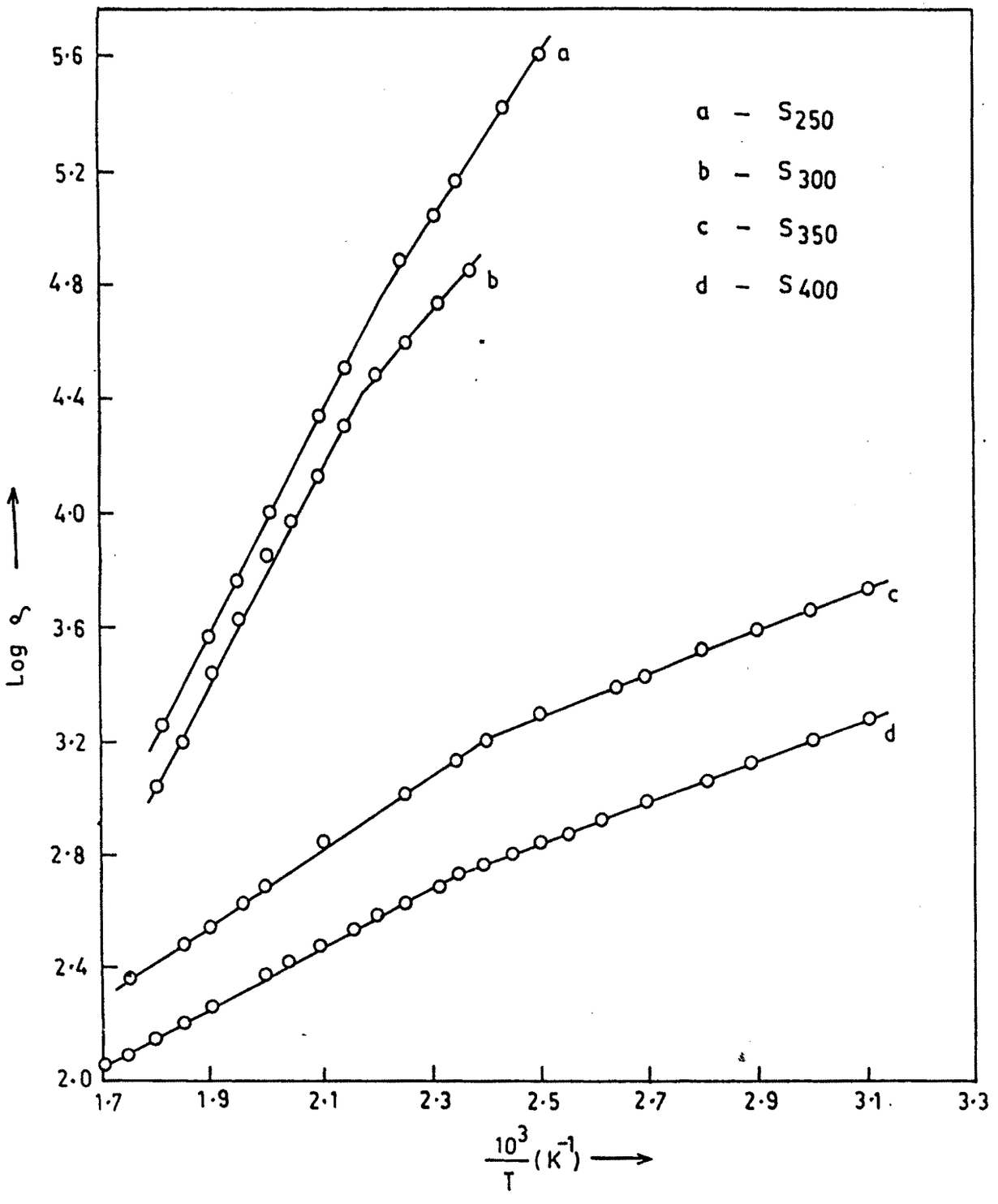

FIG. 4.10 A PLOT OF Log σ VERSUS $\frac{10^3}{T}$ FOR MoO_3 FILMS.

REFERENCES

1] D.H.Killeffer and A.Linz., Molybdenum Compounds their chemistry and technology, New York: Interscience(1952)

2] D.R.Crow, "Principls and Applications of Electrochemistry" Chapman and Hall, London (1974).

3] I.R.Weingarten and M.RothbergJ.Electrochem.Soc. 108 (1961) 167.

4] T. O.Poehler and W.Liben, Proc. IEEE 52(1964)731.

5] J.Lapage, A.Bernalte and D.A.Linholm,Rev.Sci.Instrum. 39 (1968) 1019.

6] S.C.Choo and E.L.Heasell, Rev.Sci. Instrum, 33(1963)1331

7] J.N.Bhar, Proc.IEEE 51 (1963) 1623.

8] V.K.Subashiev, Sov.Phys.Solid Stat,5(1963)405.

9] R.N.Bhattacharya and P.Pramanik,J.Electrochem.Soc.129 (1982) 332.

10] L.W.Chow, Y.C.Lei and H.L.Lwok, Thin Solid Films, 81 (1981) 307 C.

11] M.D.Uplane and S.H.Pawar, Solid State Comm.46 (1983) 847.

12] S.H.Pawar,S.P.Tamhankar and C.D.Lokhande, J.Matt.Sci. Lett. 3 (1984) 427

13] J. Zhang, S.A.Wessel and K.Colbow, Thin Solid Films, 175 (1989) 227.

14] C.G.Granqvist, Physics of Thin Films Advances in Researchand Development Mechanic and Dielectric

Properties, Vol.17,P.335, Edited by Maurice H.Francombe and John L.Vossen, (1993).

15] T.S.Moss, Optical properties of Semicoductors (Butter worth London) 1961.

16] S.K.Deb, Proc. Roy Soc. A 304 (1968) 211.

17] P.G.Dikens and D.J.Nieilf, Tran.J.Phy.Soc.64 (1968)13.

18] S.K.Krishnakumar and C.S.Menon,Bull.Mater.Sci.16 (1993) 187.

19] P.S.Nikam and H.S.Aher, Ind.J.of Pure and Appl.Phys.31 (1993) 79.